journal

J. Am. Ceram. Soc., **85** [8] 2089–96 (2002)

Effects of an Electroplated Platinum Interlayer on the Morphology and Phases of Chemically-Vapor-Deposited Alumina on Single-Crystal, Nickel-Based Superalloy

Yi-Feng Su,[†] Michele A. Torzilli,[†,‡] Justin Daniel Meyer,[†] Claudia J. Rawn,[*,§] Michael J. Lance,[*,§] Sakari Ruppi,[¶] and Woo Y. Lee[*,†]

Department of Chemical, Biochemical, and Materials Engineering, Stevens Institute of Technology, Hoboken, New Jersey 07030

Oak Ridge National Laboratory, Oak Ridge, Tennessee 37831

SECO Tools AB, S-737 82 Fagersta, Sweden

The feasibility of preparing a thin layer of α-Al_2O_3 on the surface of a single-crystal, Ni-based superalloy was examined using a chloride-based chemical vapor deposition (CVD) process previously developed for cutting tool applications. A coating directly deposited by this method on the alloy surface consisted of ~1 μm α-Al_2O_3 crystals in a matrix of amorphous Al_2O_3. When the alloy surface was predeposited with an electroplated Pt layer, the coating was mostly α-Al_2O_3, but with the presence of fine microcracks on the coating surface. In comparison to the results observed for pure Pt substrate, the role of the Pt interlayer was apparently to promote the rapid formation of κ-Al_2O_3 nuclei, which subsequently transformed to α-Al_2O_3 during the CVD growth process.

I. Introduction

THERMAL barrier coatings (TBCs) are currently used, in conjunction with air cooling, to prolong the life of metallic "hot-section" turbine components in revenue-generating aircraft engine services.[1] State-of-the-art TBCs used for rotating airfoils in aircraft engines consist of a strain-tolerant Y_2O_3-stabilized ZrO_2 (YSZ) layer prepared by electron beam physical vapor deposition (EBPVD) and a metallic bond coating which provides high-temperature oxidation protection. It is recognized that, among various failure mechanisms observed, the principal failure mode of the EBPVD-TBCs is progressive fracture along the interface region between the metallic bond coating surface and its thermally grown oxide (TGO) on oxidation and thermal cycling.[1–4] Bond coatings commonly used with the EBPVD-YSZ layer are (1) MCrAlY (where M is Ni, Co, or NiCo) prepared by vacuum plasma spray (VPS)[1] and (2) platinum aluminide prepared by Pt electroplating and subsequent aluminizing by pack cementation or chemical vapor deposition (CVD).[5]

There are some intriguing observations reported in the literature about enhancing the oxidative stability of the metal–ceramic interface by incorporating an Al_2O_3 interlayer. As reported in his patent, Strangman[6] observed that the presence of an Al_2O_3 interlayer (~1 μm) prepared by CVD between NiCoCrAlY and EBPVD-YSZ increased the TBC's burner rig life by 5 times. The increased oxidation resistance was attributed to the dense morphologic quality and high chemical purity of the CVD-Al_2O_3 layer, although the claims were made without substantial characterization results. Another independent study by Sun *et al.*[7] showed that the presence of a CVD-Al_2O_3 layer (4 μm thick) between a plasma-sprayed YSZ layer and a NiCoCrAlY layer substantially increased the cyclic oxidation life of the YSZ layer. The rate of bond coating oxidation was observed to be lower because of the presence of the CVD-Al_2O_3 layer. It was also claimed that the formation of spinels (i.e., transient oxide phases that form during the initial stage of Ni alloy oxidation) was not observed at the YSZ–TGO interface.

Both Strangman and Sun *et al.* used a CVD process which utilizes $AlCl_3$, CO_2, and H_2 as precursors at a deposition temperature of ~1000°C. This chloride-based CVD process was previously developed, and is being widely used in the cutting tool industry.[8] The non-line-of-sight, atomistic growth technique is attractive for manufacturing, since engineering components with intricate shapes and complex surface features can be readily coated. The CVD process is the only technique currently capable of commercially producing α-Al_2O_3 in the form of coherent and dense coatings in the cutting tool industry. PVD methods such as sputtering,[9] reactive sputtering,[10,11] reactive evaporation,[12] ion-assisted deposition,[13,14] and cathodic arc plasma deposition[15] are generally known to produce metastable or amorphous Al_2O_3, unless postdeposition annealing above 1000°C is applied.

In the cutting tool industry, WC/Co substrates are typically deposited with a Ti(C,N) interlayer and an "α bonding" layer before the α-Al_2O_3 deposition step. The Ti(C,N) interlayer is used as a diffusion barrier, since some of the substrate elements and impurities (particularly Co) are found to cause the formation of metastable phases or undesired morphologic features such as whiskers during the coating growth.[8,16] It has been postulated that the role of the α bonding interlayer is to promote the preferential nucleation of α-Al_2O_3 although the mechanisms are not well understood.[17,18] Another important processing feature is that air leaks into the CVD process must be tightly controlled to avoid the development of "cauliflower" growth morphology and powder formation in the gas phase. Despite these difficulties, remarkable engineering progress has been made with controlling the nucleation and growth behavior of Al_2O_3 on the cutting tool surface. For example, the selective

N. Claussen—contributing editor

Manuscript No. 187509. Received August 21, 2001; approved May 13, 2002.

This research was sponsored by the U.S. Office of Naval Research (ONR) through Grant No. N00014-99-1-0281. The luminescence and HTXRD studies were performed at Oak Ridge National Laboratory (ORNL). ORNL is managed by UT-Battelle, LLC, for the U.S. Department of Energy, under Contract No. DE-AC05-00OR22725. J. D. Meyer and M. A. Torzilli were supported in part by Robert C. Stanley Fellowships at the Stevens Institute of Technology.

[*]Member, American Ceramic Society.

[†]Stevens Institute of Technology.

[‡]Present address: Salomon Smith Barney of Citigroup, New York, New York 10013.

[§]Oak Ridge National Laboratory.

[¶]SECO Tools AB.

growth of α-Al_2O_3 or κ-Al_2O_3 (even α-Al_2O_3/κ-Al_2O_3 multilayers) is possible either by adding a small concentration ($\sim$0.1%) of $TiCl_4$ or $ZrCl_4$ as a dopant to the gas phase during the initial period of coating growth or by depositing an interlayer before the coating procedure.[8]

This paper is the first of two manuscripts prepared to address the synthesis, characterization, and performance issues associated with the α-Al_2O_3 interlayer concept. We have recently developed a novel CVD procedure for preparing a $\sim$100 nm thick layer of fully crystalline α-Al_2O_3, directly on the surface of a single-crystal, Ni-based superalloy, as described elsewhere.[19] This layer eliminated transient oxide formation and promoted the epitaxial growth of α-Al_2O_3 grains underneath the α-Al_2O_3 layer on oxidation at 1150°C. The CVD α-Al_2O_3 layer apparently reduced the number of grain boundaries in the α-Al_2O_3 scale, and consequently decreased the rate of alloy oxidation since grain boundary diffusion is the dominant transport mechanism at this temperature.

In the present paper, an industry CVD process, previously developed at SECO Tools for the cutting tool industry, was used to synthesize α-Al_2O_3 coating specimens on the (100) surface of a single-crystal Ni alloy (René N5) and on the same alloy coated with an electroplated Pt interlayer. The effects of the electroplated Pt interlayer on the nucleation and growth of the CVD α-Al_2O_3 coating were investigated for the following reasons: (i) the Pt layer, as a diffusion barrier, might mitigate the adverse effects of some alloying elements of the Ni alloy (particularly Co and Cr), which are known to cause the growth of Al_2O_3 whiskers;[8,16] (ii) beneficial effects of Pt on TGO adhesion are well known for TBC applications;[20,21] and (iii) Pt electroplating is a routine procedure for TBC production and repair. While René N5 and Pt-plated René N5 substrates were of engineering importance for this study, Pt substrate was also used to study the nucleation and growth behavior of CVD-Al_2O_3 in the absence of impurity effects. Prior studies[8,16,22] have shown that, in addition to Co and Cr impurities, Si, Fe, and Ni as well as their chlorides substantially influenced both the morphology and phase contents of the CVD-Al_2O_3 coating.

II. Experimental Procedure

(1) Substrate Materials

A single-crystal Ni alloy (René N5; René is a trademark of General Electric Co., Fairfield, CT) was cast as a cylindrical rod with the [100] seed direction. The alloy rod was sliced radially to produce disk specimens (0.2 cm thickness $\times$ 1.2 cm diameter) while preserving the (100) orientation on the disk surface. The nominal composition (in wt%) of the alloy is 6.2 Al, 0.05 C, 7.5 Co, 7.0 Cr, 0.16 Hf, 1.5 Mo, 3.0 Re, 6.5 Ta, 0.02 Ti, 5.0 W, and Ni as the balance. This alloy was melt-desulfurized to 0.8 ppmw sulfur by PCC Airfoils for Oak Ridge National Laboratory, and its oxidation characteristics have been extensively studied as described elsewhere.[23,24] The specimen surface was polished before coating experiments with 0.05 μm Al_2O_3 suspension. General Electric Aircraft Engines provided René N5 disks (0.3 cm thickness $\times$ 2.5 cm diameter) electroplated with a layer of pure Pt. The thickness of the Pt layer was nominally $\sim$7 μm. The Pt-coated alloy surface was not polished before the coating experiments. Pt substrate was cut to 10 mm $\times$ 10 mm squares from Pt foil (99.99+%, Goodfellow, Berwyn, PA). The Pt surface was not polished before the coating experiment.

(2) CVD Coating Synthesis

The CVD process at SECO Tools was used to prepare coating specimens. In this CVD process, $AlCl_3$ is generated by passing HCl over Al chips:

$$2Al(s) + 6HCl(g) \rightarrow 2AlCl_3(g) + 3H_2(g) \quad (1)$$

A CO_2 and H_2 gas mixture is used to form water vapor inside the reactor chamber via the reverse water-gas shift reaction:

$$H_2(g) + CO_2(g) \rightarrow H_2O(g) + CO(g) \quad (2)$$

Subsequently $AlCl_3$ and H_2O react as follows:

$$2AlCl_3(g) + 3H_2O(g) \rightarrow Al_2O_3(s) + 6HCl(g) \quad (3)$$

The overall reaction for the CVD-Al_2O_3 process is

$$2AlCl_3(g) + 3H_2(g) + 3CO_2(g) \rightarrow Al_2O_3(s) + 6HCl(g) + 3CO(g) \quad (4)$$

The *in situ* generation of H_2O (Eq. (2)) is preferred because the H_2/CO_2 gas mixture is relatively stable in high-temperature environments, and therefore can act as a water reservoir.[8] This effect is used to increase the deposition zone, allowing for more uniform coating deposition over large and complex substrate geometries. Additionally, as the rate-determining step of the overall reaction (Eq. (4)), the reverse water-shift reaction (Eq. (2)) serves as a mechanism for controlling the growth rate of Al_2O_3. However, if H_2O were introduced directly into the reaction chamber, there would be homogeneous nucleation in the vapor phase near the gas inlet, resulting in powder formation and incomplete reaction products (e.g., AlO_xCl_y).[25]

Coating specimens were prepared using the general procedure described elsewhere.[26] Table I shows the process conditions used for the coating experiment. It is important to note that the substrates were pretreated with $AlCl_3$ and H_2 for 1 min before adding CO_2 to start the CVD-Al_2O_3 procedure.

(3) Characterization Methods

Coating morphology and compositions were examined using a field emission scanning electron microscope (SEM, LEO 982, LEO Electron Microscopy, Inc., Thornwood, NY) equipped with an energy dispersive spectroscopy (EDS). An Au–Pd layer was sputtered on the sample surface along with the use of carbon tape and silver paste to minimize the charging problems associated with the nonconductive Al_2O_3 coating. Surface and cross-section elemental distributions, as measured by EDS, were used to determine the phase distribution in the CVD-Al_2O_3 coating samples. The cross-section images were prepared by conventional metallographic techniques. Phase contents of the coating specimens were studied by X-ray diffraction (XRD, Siemens Diffractometer D5000, Bruker AXS, Inc., Madison, WI) with capability to perform grazing incidence XRD (GIXRD) measurements. The GIXRD technique was useful for analyzing the coating layer while reducing contributions from the substrate peaks, as the incident angle provided a very shallow penetration depth into the sample.[27]

In addition to XRD, luminescence spectroscopy was used to determine the presence of the α-Al_2O_3 phase in the coating layer as well as to measure the average hydrostatic stress of the α-Al_2O_3 phase in the coating layer. α-Al_2O_3 has trigonal symmetry with rhombohedral Bravis centering[28] and can possess a trace amount of Cr^{3+} cations.[29–31] The Cr^{3+} cations, having the same valence as Al^{3+}, substitute for them in the α-Al_2O_3 crystal lattice. When excited by a laser, the electrons of the Cr^{3+} emit photons. The two characteristic photon energies for the α-Al_2O_3 phase are 14 402 cm^{-1} (R1) and 14 432 cm^{-1} (R2). In contrast, other metastable alumina phases do not exhibit fluorescence peaks except for θ-Al_2O_3 and γ-Al_2O_3 phases.

When there is a stress in the α-Al_2O_3 phase, there is a physical shifting of the lattice as a whole and the relative positions of the

Table I. Deposition Conditions Used for the CVD Alumina Experiment

Temperature (°C)	1020
Total pressure (kPa)	30
H_2 (vol%)	Balance
CO_2 (vol%)	3.3
$AlCl_3$ (vol%)	4.2
Duration (h)	3

oxygen and chromium ions in particular. This shifting changes the electronic environment of the chromium and there is a corresponding shift in the R1 and R2 lines.[29–31] In this work, a Dilor XY 800 triple-stage Raman micropobe and a coherent Innova 308C argon ion laser operating at 514.5 nm with a 100 mW output power were used. The laser was focused onto areas of interest with an optical objective providing a spatial resolution of 2 or 10 μm, depending on the objective used.

III. Results

(1) René N5

SEM/EDS, XRD, and luminescence data suggested that the CVD-Al_2O_3 coating directly deposited on René N5 was essentially made of ~1 μm in average α-Al_2O_3 crystals in a matrix of amorphous Al_2O_3. As shown in Fig. 1(a), the coating surface consisted of two distinct features: (i) faceted crystals of ~0.5–1.5 μm and (ii) a glassy, weblike feature which surrounded the faceted crystals. The coating surface was not fully "dense" because of the lack of coalescence among the crystals and the presence of the glassy phase between the crystals. As shown in Fig. 2(a), the coating was ~1 μm thick, and contained Al and O only when examined by EDS.

The XRD patterns in Fig. 3 suggested that the coating contained α-Al_2O_3 crystals with random crystal orientation as the only crystalline phase in the coating. The GIXRD pattern (Fig. 3(b)) showed that the top region of the coating layer was mostly α-Al_2O_3. At first glance, the penetration of the XRD beam through the coating sample appeared to be relatively small, as the substrate peak was barely visible from the normal XRD shown in Fig. 3(a). Significant broadening of the base line was observed. The high background could be attributed to the presence of some amorphous content in the coating layer as well as amorphorization of the substrate region just beneath the coating layer, although a more definitive assessment was not be possible with the XRD analysis.

It should be noted that the high background could also be the result of Ni fluorescing from the superalloy on exposure to X-ray radiation, since Ni is close to Cu in terms of radiation. However, the high background was not observed during the X-ray analysis of uncoated Ni alloy and pure Ni substrates. As reported in an earlier paper[32] and shown in Fig. 3(c), the high background disappeared on vacuum annealing and oxidation in a high-temperature XRD chamber at temperatures up to 1200°C for 1 h. Also, the α-Al_2O_3 peaks became much stronger at the expense of the broad base line, along with several peaks which could not be indexed. These results further indicated that the coating contained a substantial amount of the amorphous Al_2O_3 phase which was transformed to the α phase during the subsequent HTXRD measurements.

As shown in Fig. 4, very broad R1 and R2 fluorescence peaks were observed for the coating sample with the 10-μm Raman probe. The presence of γ- or θ-Al_2O_3 was not observed. Further analysis with the 2-μm probe suggested that the crystals (0.5–1.5 μm) observed in the SEM micrograph (Fig. 1(a)) were α-Al_2O_3, as evidenced by sharpening of the R1 and R2 peaks. The luminescence peaks became weaker in the glassy areas of the coating surface, suggesting that these regions of the coating layer were amorphous.

The average stress in the coating layer was measured to be −3.2 GPa. Because of the coefficient of thermal expansion (CTE) mismatch between the α-Al_2O_3 coating and the René N5 substrate, the compressive residual stress was expected to develop in the in-plane direction of the coating layer on cooling from the CVD deposition temperature to room temperature. The broadness of the

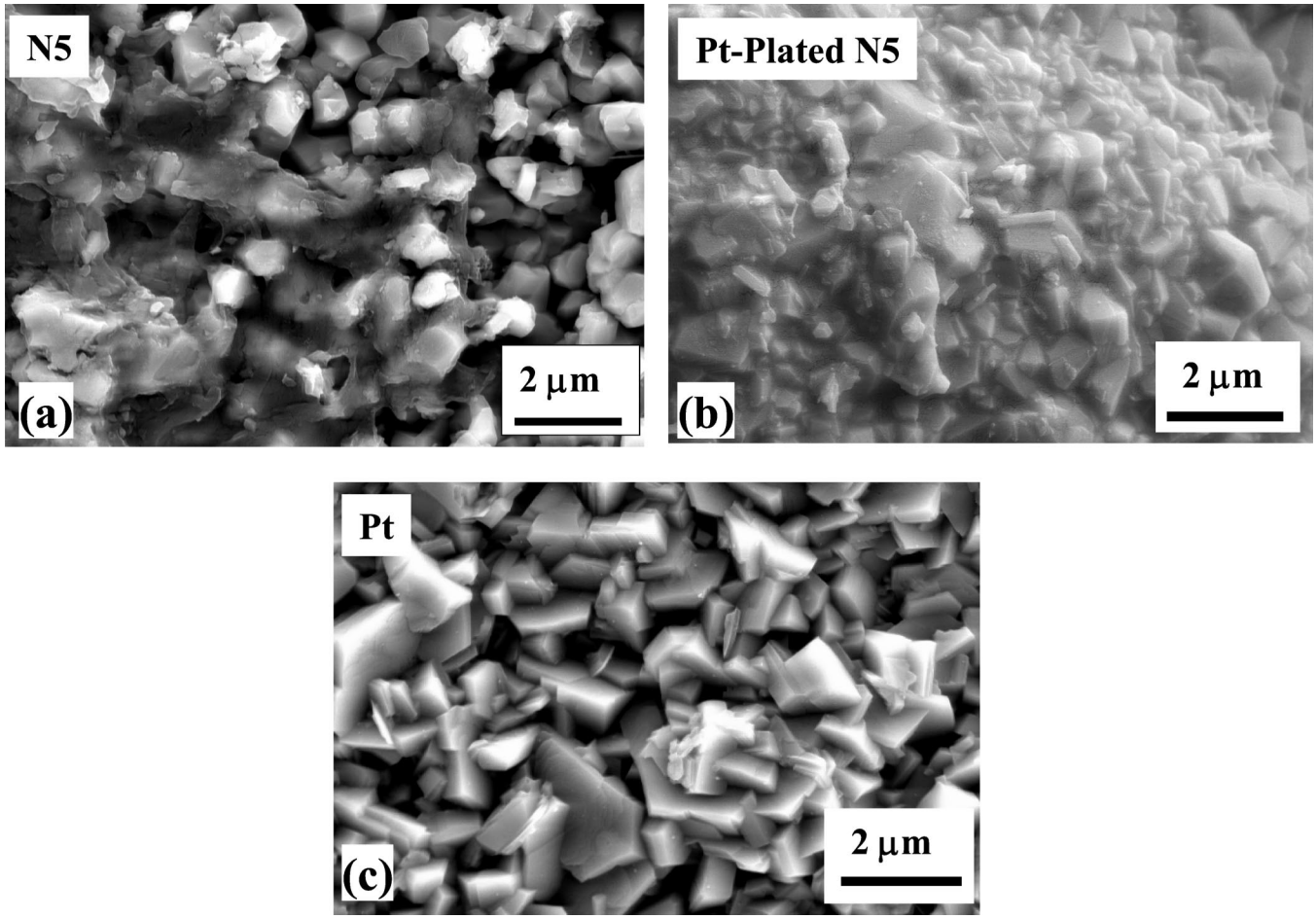

Fig. 1. Surface SEM images of as-deposited CVD-Al_2O_3 coating deposited on (a) René N5, (b) Pt-plated René N5, and (c) pure Pt.

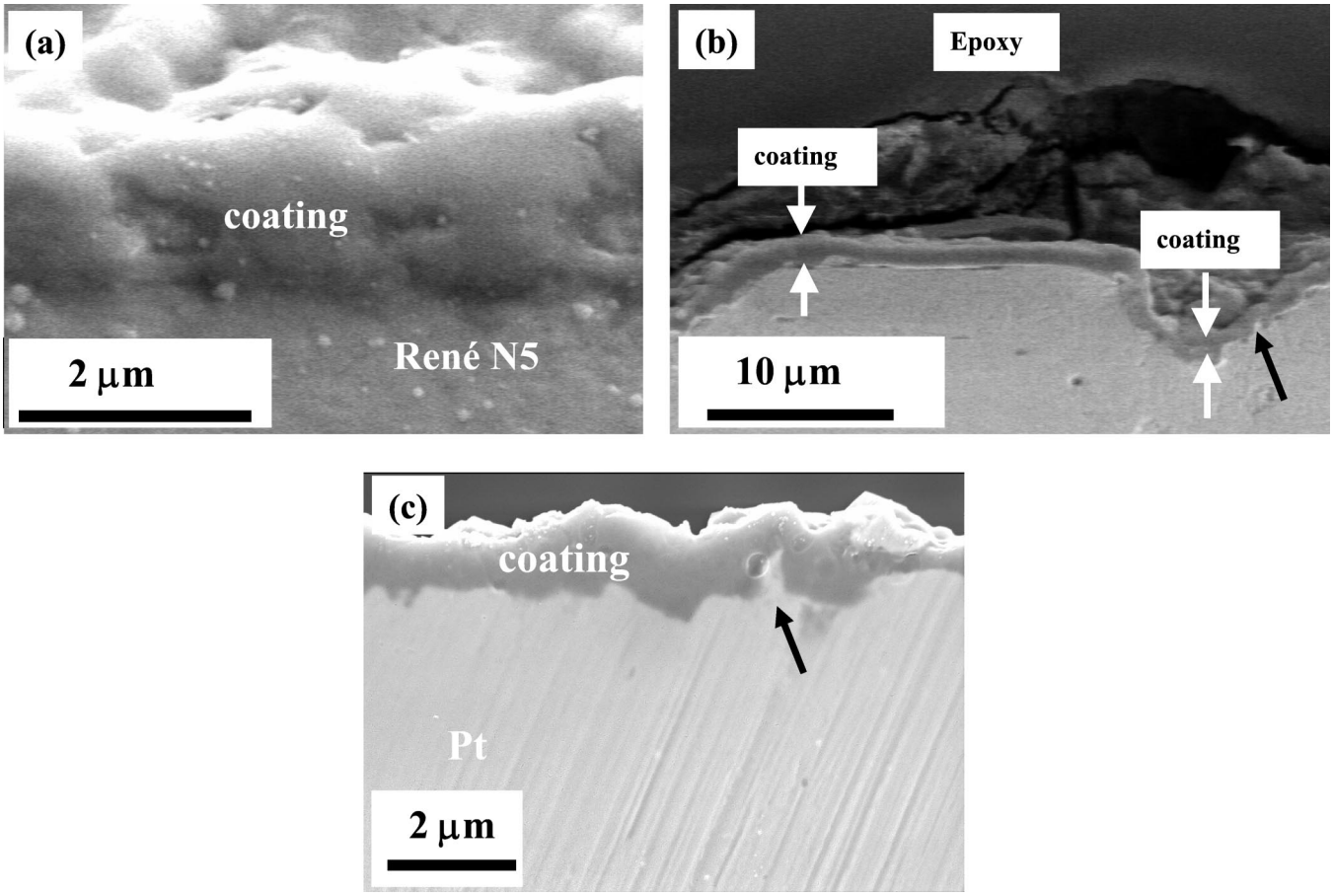

Fig. 2. Cross-section SEM images of CVD-Al_2O_3 deposited on (a) Rene N5, (b) Pt-plated René N5, and (c) pure Pt.

R1 and R2 suggested that there were strain gradients existing within the probed volume of the α-Al_2O_3 crystals.[30]

(2) Pt-Plated René N5

The surface of the alumina coating deposited on the Pt-plated René N5 substrate was not uniform, as characterized by the presence of ~20 μm "rumples" on the coating surface (Figs. 2(b) and 5(a)), which originated from the Pt plating process. On the surface of each rumple surface, Al_2O_3 crystals of ~0.1 to 1 μm were clearly visible (Figs. 1(b) and 5(b)). The crystals (0.5–1.5 μm) were α-Al_2O_3 as examined by luminescence spectroscopy. The presence of the γ- and θ-Al_2O_3 was not detected by this characterization method. At higher magnifications, an array of very fine microcracks (~100 nm) appeared on the coating surface, particulary in the "valley" regions between the Al_2O_3 crystals (Fig. 5(b)). Despite the presence of these microcracks, the coating layer was found to be highly compressed by the luminescence spectroscopy with the average stress of −3.2 GPa (Fig. 4).

In cross-sectional view of the sample, the coating was found to be ~2 μm thick, and contained small metallic protrusions from the substrate into the coating layer (as indicated by the black arrow in Fig. 2(b)). From the literature on high-temperature oxidation, it has been documented that this type of "pegging" behavior is known to occur during the oxidation of Pt-modified aluminide coatings, and is viewed as one of the mechanisms by which Pt improves alumina scale adhesion.[33,34] It has also been reported that Pt would work as a filter/barrier[33,35] that inhibits outward diffusion of the refractory elements. Our SEM/EDS analysis did not show the presence of any elements other than Al, O, and Pt in the coating layer, supporting the role of Pt as a diffusion barrier.

In contrast to the coating directly deposited on René N5, no high background in the XRD pattern was observed. The XRD spectrum (Fig. 6) showed that the coating was predominately α-Al_2O_3 with

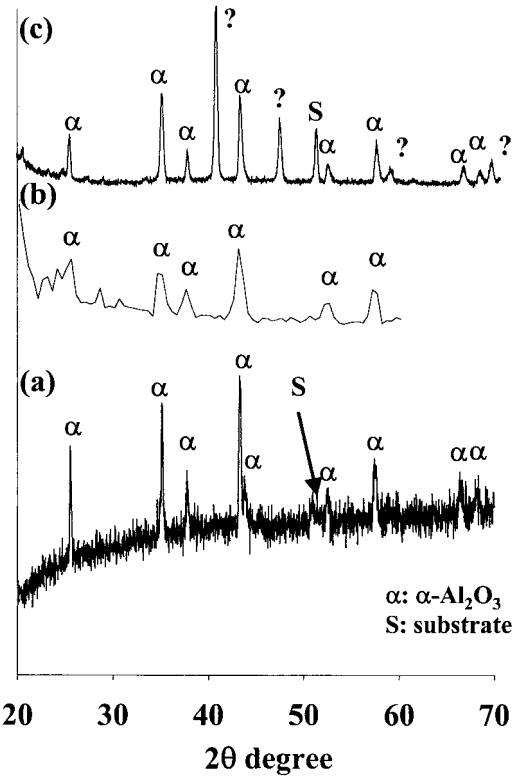

Fig. 3. XRD patterns of CVD-Al_2O_3 on Rene N5: (a) normal scan, (b) 1° grazing incident, (c) normal scan after oxidation with air at 1200° for 1 h.

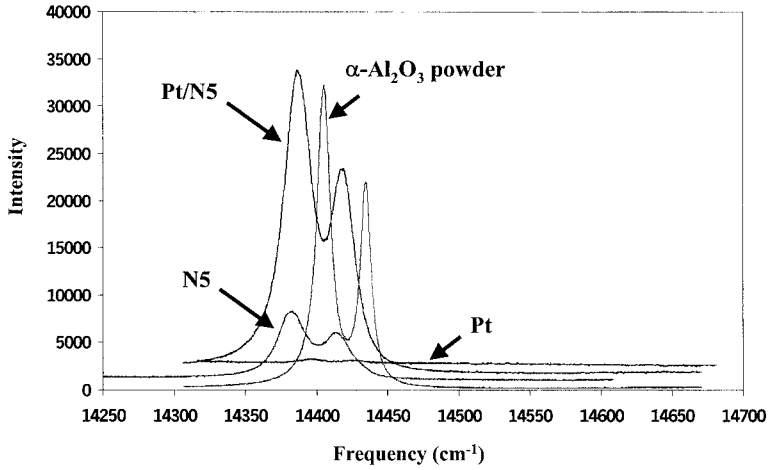

Fig. 4. Luminescence spectra of CVD-Al_2O_3 on Rene N5 (N5), Pt-plated René N5 (Pt/N5), and pure Pt (Pt) in comparison to that of stress free α-Al_2O_3 powder.

a trace of κ-Al_2O_3. The intensity of substrate peaks in the XRD pattern for this sample was significant. As described earlier, in contrast, the substrate peak from the coating deposited on René N5 (Fig. 4(a)) was very weak with the appearance of the high background. Since the thickness of the coating deposited on both substrates was similar, our interpretation of the amorphorization of the substrate/coating interface region appeared to be reasonable.

(3) Pure Pt

The SEM image in Fig. 1(c) shows that the surface of the coating deposited on Pt was highly faceted with polygonal platelets of ~0.5 μm in size and without any microcracking. From the cross-sectional image in Fig. 2(c), the as-deposited coating layer was estimated to be ~1 to 2 μm thick. Also, from the image, metallic protrusions from substrate into the coatings were observed (as indicated by the black arrow in Fig. 2(c)), as a similar "pegging" behavior was observed with the Pt-plated René N5 sample.

The majority of the dominant XRD peaks (Fig. 7) were indexed to Pt_3Al. The minor peaks in the XRD pattern were assigned to κ-Al_2O_3. It has been reported that Pt rapidly reacts with aluminum during aluminizing,[36] eventually to form Pt_3Al as the reaction product in our coating. This might explain the formation of Pt_3Al as an interlayer between the Al_2O_3 layer and the substrate. However, there was no evidence for Pt_3Al formation for the coating formed on Pt-plated René N5. As reported by Krishna *et al.*,[36] the thickness of the initial Pt layer could be a factor which affected the Al uptake and Pt_3Al phase formation behaviors. As shown in Fig. 4, luminescence measurements showed the presence of very small R1 and R2 peaks above the background. Their low intensity indicated that the amount of α-Al_2O_3 was very small, and therefore the XRD analysis was unable to detect this minute amount. There were no measurable shifts in the R1 and R2 lines for this sample.

IV. Discussion

The characterization results, as summarized in Table II, clearly showed the strong effects of substrate on the phase contents and morphology of the CVD-Al_2O_3 coating. It is well known that the effects of substrates on the nucleation and growth of CVD materials could be significant,[37] particularly for Al_2O_3.[38] In this section, we will compare our observations to those reported in the literature to comprehend the apparent effects of the Pt interlayer on the nucleation and growth behavior of CVD-Al_2O_3.

The surface morphology and phase contents of the coating specimens produced on René N5 and Pt-plated René N5 were quite different. The coating produced on René N5 consisted of α-Al_2O_3 crystals of ~0.5–1.5 μm in a glassy, discontinuous matrix phase of amorphous Al_2O_3. On the other hand, the coating on Pt-plated René N5 contained α-Al_2O_3 crystals of ~0.1 to 1 μm and with a minute amount of κ-Al_2O_3. Another major difference was the presence of very fine microcracks (~100 nm) on the coating surface of the Pt-plated René N5 sample particularly in the

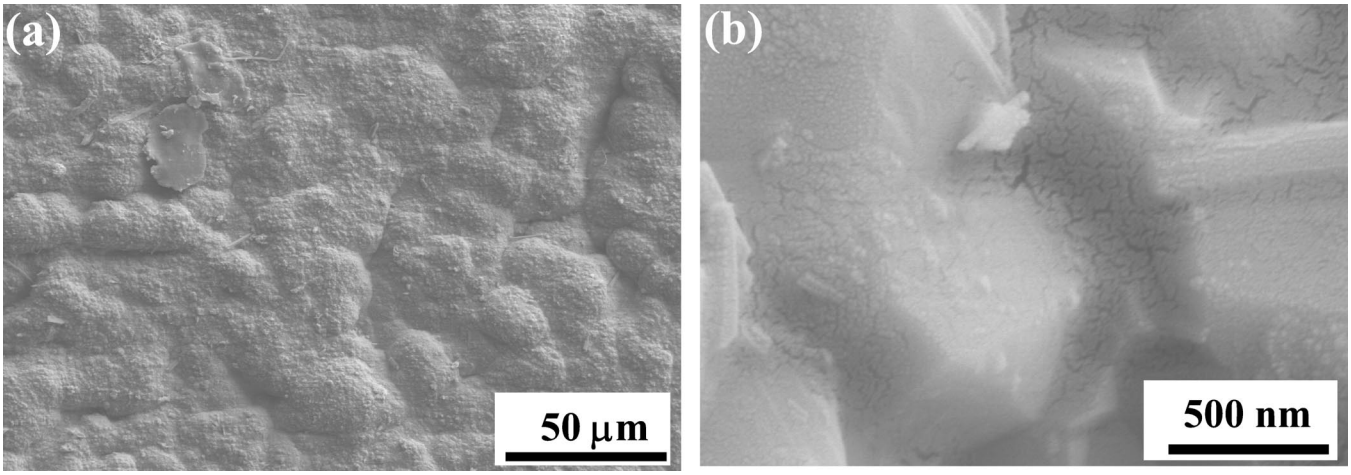

Fig. 5. Surface SEM images of CVD-Al_2O_3 on Pt-plated N5: (a) as-deposited, and (b) fine microcracks appeared at higher magnification.

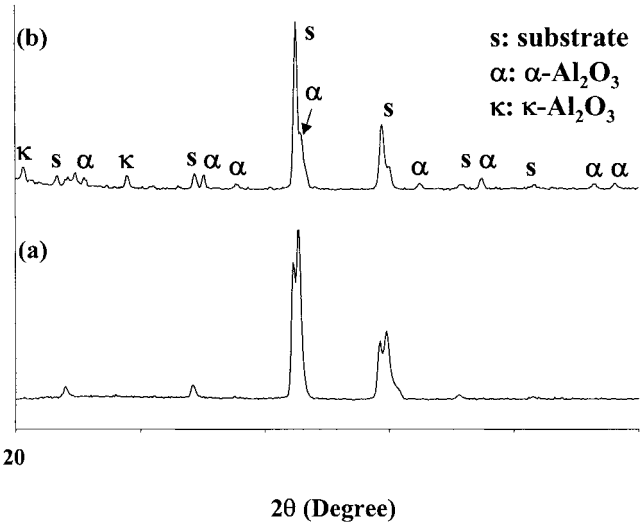

Fig. 6. XRD patterns of Pt-plated René N5: (a) before and (b) after CVD-Al_2O_3.

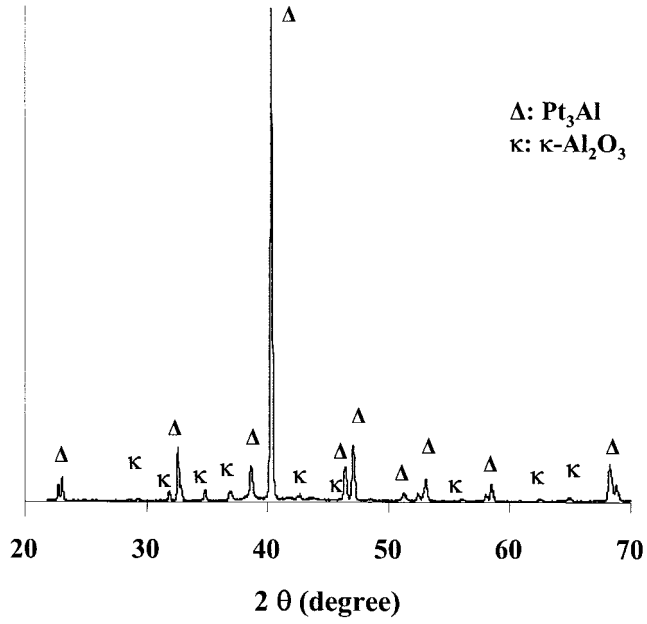

Fig. 7. XRD pattern of the as-deposited CVD coating on pure Pt.

"valley" regions between the Al_2O_3 (Fig. 5(b)). To understand the appearance of microcracks, we will need to consider the results observed for the pure Pt substrate.

For the Pt-plated René N5 and pure Pt substrates, their surface morphologies were seemingly similar at first glance. However, the XRD and luminescence results indicated that the coating on the pure Pt substrate was predominantly κ-Al_2O_3 with a very small amount of α-Al_2O_3 whereas the coating deposited on the pure Pt substrate did not exhibit microcracking. The appearance of microcracks suggested that the κ- to α-Al_2O_3 transformation had occurred within the coating layer deposited on Pt-plated René N5 during the CVD step and/or possibly the cooling period. κ- to α-Al_2O_3 transformation has been commonly observed during the CVD-Al_2O_3 process.[28] For example, it was previously reported that α-Al_2O_3 tended to form as larger grains surrounded by fine κ-Al_2O_3 grains and with microcracks during the CVD process.[8] The microcracking is caused by the volume shrinkage (~8 vol%) associated with the κ- to α-Al_2O_3 phase transformation, as calculated from the κ- and α-Al_2O_3 structure data.[39] As reported elsewhere,[32] we also observed the development of microcracking when the coating on the pure Pt substrate was transformed from κ to α within 12 min on annealing at 1250°C by high-temperature XRD.

The XRD and EDS analyses showed that a Pt_3Al layer of a few micrometers probably formed underneath the κ-Al_2O_3 layer on the pure Pt substrate. The formation of the Pt_3Al layer could be attributed to the pretreatment procedure in which the substrates were exposed to the $AlCl_3 + H_2$ mixture for 1 min before starting the Al_2O_3 deposition. As noted earlier, the procedure is used to create a "bonding" layer for the TiC, TiN, Ti(C,N), or Ti(C,N)/(WC/Co) surfaces for cutting. This "prealuminizing" procedure might have aluminized the surface of the pure Pt substrate and formed the Pt_3Al phase. However, there was no evidence for Pt_3Al formation for the coating formed on Pt-plated René N5. As reported by Krishna *et al.*,[36] the thickness of the initial Pt layer could be a factor which affected the amount of Al uptake and therefore the formation of the Pt_3Al phase and its interdiffusion with the René N5 substrate.

Apparently, the Pt substrate was able to promote the formation of κ-Al_2O_3. However, from the crystallographic point of view, there is no relationship between Pt (cubic) or Pt_3Al (tetragonal) and κ-Al_2O_3 (orthorhombic). Halvarsson *et al.* previously observed that there were no particular crystallographic correlations between the "bonding" layers and the selection of α or κ phase.[18] Nevertheless, our results are in agreement with prior observations by Vuorinen *et al.*[17,18,38] that phase contents in the CVD-Al_2O_3 coating are strongly dictated by the interlayer(s) that forms beneath the CVD layer.

The "pegging" behavior, as characterized by metallic protrusions into the alumina coating layer, was observed for pure Pt and Pt-plated René N5, but not from René N5. Therefore, the results suggested that the "pegging" behavior occurred where Pt was present. Interestingly, our observations were in agreement with the "pegging" behavior of Pt observed in the oxidation of Pt-modified aluminide coatings. This behavior is viewed as one of the mechanisms by which Pt improves alumina scale adhesion.[33,34]

In contrast to the coatings on the pure Pt and Pt-plated René N5 substrates, the coating deposited on René N5 contained a significant amount of the amorphous Al_2O_3 phase in addition to the α-Al_2O_3. It appeared that some alloying elements in René N5 might have certain effects on the formation of the amorphous phase. Levin *et al.*[28] indicated that with the presence of Ni^{2+} ions, metastable to α transformation would be retarded. However, with the available data, we were not able to address the mechanism by which the amorphous and α-Al_2O_3 phases coexisted in the coating formed on René N5. However, as Fig. 3(c) shows, the amorphous content of the coating (or in the coating/substrate interface region) crystallized rapidly on exposure to 1200°C.

As summarized in Table II, the average compressive stress (−3.2 GPa) was measured for the coating on René N5 (Fig. 4). The compressive stress could be attributed to the residual stress, which resulted from the CTE mismatch between the René N5 ($\sim 13.1 \times 10^{-6}$/°C) and the Al_2O_3 coating (8×10^{-6}–9×10^{-6}/°C) during cooling from the deposition temperature of 1050°C to room temperature. This stress value is within the range of various stress values reported for alumina scales formed on superalloys on high-temperature oxidation.[30] Interestingly, even with the presence of microcracks on the surface of the alumina coating on Pt-plated René N5, the stress level was the same as that measured for the coating deposited directly on René N5. It seemed that these microcracks were not sufficiently large to form a continuous network to release the stress.

V. Conclusions

The Al_2O_3 CVD process, previously developed at SECO Tools for coating WC/Co cutting tools, was used to synthesize Al_2O_3

Table II. Major Phases Detected by XRD and Luminescence Spectroscopy and the Average Stress Measured from the α-Al_2O_3 Phase in the CVD Coating

Substrate	Growth rate (mg/(cm^2·min))	Phases	Stress (GPa)
René N5	0.0132	α + amorphous	−3.2
Pt-plated René N5	0.0186	α + κ (trace)	−3.2
Pure Pt	0.0116	Pt_3Al + κ + α (trace)	0

coating specimens on René N5, René N5 coated with an electroplated Pt interlayer, and pure Pt substrates. The characterization results showed that the phase contents and morphology of the CVD-Al_2O_3 coating were strongly dictated by the substrates. The coating directly deposited on René N5 consisted of α-Al_2O_3 crystals of ~0.5–1.5 μm in a glassy, discontinuous matrix phase of amorphous Al_2O_3. On the other hand, the coating on Pt-plated René N5 contained α-Al_2O_3 crystals of ~0.1 to 1 μm and with a minute amount of κ-Al_2O_3. The coating on pure Pt was κ-Al_2O_3 along with a trace amount of α-Al_2O_3, but with the formation of a major amount of Pt_3Al at the coating/substrate interface. The average stress values measured for the coatings on René N5 and Pt-plated René N5 were within the range of various stress values reported for alumina scales formed on superalloys and Pt-modified coatings on high-temperature oxidation, which suggested that adhesion at the coating/substrate was excellent for both specimens.

The appearance of fine microcracks suggested that the κ- to α-Al_2O_3 transformation occurred within the coating layer deposited on Pt-plated René N5 during the CVD step. Apparently, the presence of Pt in the Pt-plated substrate, as in the case of the pure Pt substrate, promoted the formation of κ-Al_2O_3. However, from a crystallographic point of view, there is no known relationship between Pt (or Pt_3Al) and κ-Al_2O_3. Nevertheless, our results were consistent with other investigators' observations that phase contents in the CVD-Al_2O_3 coating were sensitive to an interlayer(s) that forms at the interface between the CVD layer and substrate without any crystallographic relationship. These results suggested that the preparation of α-Al_2O_3, as an entirely homogeneous and fully dense layer without microcracks, on the Ni superalloy surface would be difficult via simple adaptation of the chloride-based CVD process and the use of a Pt interlayer. The extent of morphologic tailoring that may be possible via other surface modification methods is currently being investigated.

Acknowledgments

We are grateful to Dr. Steven Fishman at the Office of Naval Research for his support and encouragement. We also thank Dr. Ram Darolia at General Electric Aircraft Engines, who has provided an industrial perspective on our research goals and progress.

References

[1]J. T. DeMasi-Marcin and D. K. Gupta, "Protective Coatings in the Gas Turbine Engine," *Surf. Coat. Technol.*, **68** [69] 1–9 (1994).

[2]R. V. Hillery *et al*., "Coating for High Temperature Structural Materials: Trends and Opportunities," National Materials Advisory Board Report, Nation Academy Press, Washington, DC, 1996.

[3]W. Y. Lee, D. P. Stinton, C. C. Berndt, F. Erdogan, Y. D. Lee, and Z. Mutasim, "Concept of Functionally Graded Materials for Advanced Thermal Barrier Coating Applications: A Review," *J. Am. Ceram. Soc.*, **79** [12] 3003–12 (1996).

[4]S. M. Meier, D. M. Nissley, K. D. Sheffler, and T. A. Cruse, "Thermal Barrier Coating Life Prediction Model Development," *Trans. ASME*, **114**, 258–63 (1992).

[5]E. C. Duderstadt and B. A. Nagaraj, U.S. Pat. No. 5 238 752, 1993.

[6]T. E. Strangman, "Ceramic Thermal Barrier Coating with Alumina Interlayer" U.S. Pat. No. 4 880 614, 1990.

[7]J. H. Sun, E. Chang, C. H. Chao, and M. J. Cheng, "The Spalling Modes and Degradation Mechanism of ZrO_2–8 wt% Y_2O_3/CVD-Al_2O_3/Ni-22Cr-10Al-1Y Thermal Barrier Coating," *Oxid. Met.*, **40**, 465–81 (1993).

[8]E. Fredriksson and J.-O. Carlsson, "Chemical Vapor Deposition of Aluminum Oxides from Various Gas Mixtures," *J. Chem. Vapor Dep.*, **1**, 333–417 (1993).

[9]M. K. Smit, G. A. Acekt, and C. J. van de Lann, "Al_2O_3 Films for Integrated Optics," *Thin Solid Films*, **138** [2] 171–81 (1986).

[10]H. K. Pulker, W. Haag, M. Buhler, and E. Moll, "Properties of Ion Plated Oxide Films," *J. Vac. Sci. Technol. A*, **3** [6] 2700–701 (1985).

[11]T. C. Chou, D. Adamson, J. Mardinly, and T. G. Nieh, "Microstructural Evolution and Properties of Nanocrystalline Alumina Made by Reactive Sputtering Deposition," *Thin Solid Films*, **205**, 131–39 (1991).

[12]A. Feldman, E. N. Farabaugh, and Y. N. Sun, "Stoichiometry of Reactively Evaporated Films"; pp. 14–17 in Optical Society of America Technical Digest Series, Vol. 6, *Optical Interference Coatings* (summaries of papers presented at the Optical Interference Coatings Topical Meeting, Tucson, AZ, April 12–15, 1988). Optical Society of America, Washington, DC, 1988.

[13]R. S. Bhattacharya, A. K. Rai, and A. W. McCormick, "Ion Beam Assisted Deposition of Al_2O_3 Thin Films," *Surf. Coat. Technol.*, **46** [2] 155–63 (1991).

[14]M. S. Al-Robaee, M. G. Krishna, G. N. Subanna, K. N. Rao, and S. Mohan, "Properties of Al_2O_3 Films Prepared by Argon Ion Assisted Deposition," *J. Mater. Res.*, **9** [10] 2668–94 (1994).

[15]T. D. Schemmel, R. L. Cunningham, and H. Randhawa, "Process for High-Rate Deposition of Al_2O_3," *Thin Sold Films*, **181**, 597–601 (1989).

[16]H. Alltena, C. Colombier, A. Lebl, J. Lindström, and B. Lux, "Formation of Whiskers on Al_2O_3 CVD Layers"; pp. 428–34 in Proceedings of the 4th European Conference on Chemical Vapor Deposition. Edited by J. Bloem, G. Verspui, and L. R. Wolff. The Centre, Eindhoven, Netherlands, 1983.

[17]S. Vuorinen and J. Skogsmo, "Characterization of α-Al_2O_3, κ-Al_2O_3, and α–κ Multioxide Coating on Cemented Carbides," *Thin Solid Films*, **193** [194] 536–46 (1990).

[18]M. Halvarsson, H. Nordén, and S. Vuorinen, "The Microstructure of Bonding Layers for CVD Alumina Coatings," *Surf. Coat. Technol.*, **68** [69] 266–73 (1994).

[19]Y.-F. Su, J. D. Meyer, L. M. He, M. J. Lance, and W. Y. Lee, "Effects of Alpha-Al_2O_3 Nanotemplate on the Oxidation Behavior of an Alumina-Forming Ni-Based Superalloy," submitted to *Metall. Trans. A*.

[20]Y. Zang, W. Y. Lee, J. A. Haynes, I. G. Wright, B. A. Pint, K. M. Cooley, and P. K. Liaw, "Synthesis and Cyclic Oxidation Behavior of a (Ni,Pt)Al Coating on a Desulfurized Ni-Based Superalloy," *Metall. Trans. A*, **30A**, 2679–87 (1999).

[21]J. A. Haynes, Y. Zhang, W. Y. Lee, B. A. Pint, I. G. Wright, and K. M. Cooley, "Effects of Platinum Additions and Sulfur Impurities on the Microstructure and Scale Adhesion Behavior of Single-Phase CVD Aluminide Bond Coatings"; pp. 185–96 in *Elevated Temperature Coatings: Science and Technology III*. Edited by J. M. Hampikian and N. B. Dahotre. The Minerals, Metals, and Materials Society, San Diego, CA, 1999.

[22]B. Lux, C. Colombier, H. Altena, and K. Stjernberg, "Preparation of Alumina Coatings by Chemical Vapor Deposition," *Thin Solid Films*, **138** [1] 49–64 (1986).

[23]I. G. Wright, P. A. Pint, W. Y. Lee, K. B. Alexander, and K. Prüβner, "Some Effects of Metallic Substrate Composition on Degradation of Thermal Barrier Coatings"; pp. 95–113 in *High Temperature Surface Engineering*. IOM Communications, London, U.K., 2000.

[24]B. A. Pint, I. G. Wright, W. Y. Lee, Y. Zhang, K. Prüβner, and K. B. Alexander, "Substrate and Bond Coat Compositions: Factors Affecting Alumina Scale Adhesion," *Mater. Sci. Eng. A*, **A245**, 201–11 (1998).

[25]P. Wong and M. Robinson, "Chemical Vapor Deposition of Polycrystalline Al_2O_3," *J. Am. Ceram. Soc.*, **53** [11] 617–21 (1970).

[26]S. Ruppi and A. Larsson, "Chemical Vapor Deposition of κ-Al_2O_3," *Thin Solid Films*, **388**, 50–61 (2001).

[27]A. J. Perry, D. E. Geist, A. F. Tian, J. R. Treglio, and K. Narasimhan, "Diffraction Pattern Indexing and the Effect of Metal Ion Implantation on κ-Alumina," *Surf. Coat. Technol.*, **89**, 62–69 (1997).

[28]I. Levin and D. Brandon, "Metastable Alumina Polymorphs: Crystal Structures and Transition Sequences," *J. Am. Ceram. Soc.*, **81** [8] 1995–2012 (1998).

[29]G. Gregori, W. Burger, and V. Sergo, "Piezospecstroscopic Analysis of the Residual Strsses in Zirconia-Toughened Alumina Ceramics: The Influence of the Tetragonal-to Monoclinic Transformation," *Mater. Sci. Eng.*, **A271**, 401–406 (1999).

[30]D. R. Clarke, R. J. Christensen, and V. T. Tolpygo, "The Evolution of Oxidation Stresses in Zirconia Thermal Barrier Coated Superalloy Leading to Spalling Failure," *Surf. Coat. Technol.*, **94** [95] 89–93 (1997).

[31]J. He and D. R. Clarke, "Determination of the Piezospectroscopic Coefficients for Chromium-Doped Sapphire," *J. Am. Ceram. Soc.*, **78** [5] 1347–53 (1995).

[32]Y.-F. Su, M. Torzilli, J. D. Meyer, W. Y. Lee, C. J. Rawn, M. J. Lance, and S. Ruppi, "Synthesis of α-Al_2O_3 Template on Ni Superalloy Surface by Chemical Vapor Deposition"; pp. 15–28 in *Elevated Temperature Coatings: Science and Technology IV*. Edited by N. B. Dahotre, J. M. Hampikian, and J. E. Morral, The Minerals, Metals, and Materials Society, Warrendale, PA, 2001.

[33]Y. Zhang, "Effect of Sulfur Impurities and Platinum Incorporation on the

Oxidation of Aluminide Coatings Synthesized by Chemical Vapor Deposition"; Ph.D. Thesis. University of Tennessee, Knoxville, TN, 1998.

[34]Y. Zhang, J. A. Haynes, W. Y. Lee, I. G. Wright, B. A. Pint, K. M. Cooley, and P. K. Liaw, "Effects of Pt Incorporation on the Isothermal Oxidation Behavior of Chemical Vapor Deposition Aluminide Coatings," *Metall. Trans. A*, **32** [7] 1727–41 (2001).

[35]H. M. Tawancy, N. Sridhar, N. M. Abbas, and D. Rickerby, "Comparative Thermal Stability Characteristics and Isothermal Oxidation Behavior of an Aluminided and a Pt-Aluminized Ni-Based Superalloy," *Scr. Metall. Mater.*, **33**, 1431–38 (1995).

[36]G. R. Krishna, D. K. Das, V. Singh, and S. V. Joshi, "Role of Pt Content in the Microstructural Development and Oxidation Performance of Pt-Aluminide Coatings Produced Using a High-Activity Aluminizing Process," *Mater. Sci. Eng.*, **A251**, 40–47 (1998).

[37]W. Y. Lee, "Effects of Initial Substrate Surface on Microstructure of Si_3N_4 Deposited by LPCVD"; pp. 665–68 in Materials Research Society Symposium Proceedings, Vol. 280, *Evolution of Surface and Thin Film Microstructure*. Edited by H. A. Atwater, E. Chason, M. H. Grabow, and M. G. Lagally. Materials Research Society, Pittsburgh, PA, 1993.

[38]M. Halvarsson and S. Vuorinen, "The Influence of the Nucleation Surface on the Growth of CVD α-Al_2O_3 and κ-Al_2O_3," *Surf. Coat. Technol.*, **76** [77] 287–96 (1995).

[39]M. Halvarsson, V. Langer, and S. Vuorinen, "X-ray Powder Diffraction Data for κ-Al_2O_3," *J. Powder Diffr.*, **14** [1] 61–64 (1999). □